NAVAL POSTGRADUATE SCHOOL

MONTEREY, CALIFORNIA

THESIS

ORBIT DETERMINATION OF HIGHLY ECCENTRIC ORBITS USING A RAVEN TELESCOPE

by

Michael L. Thrall

September 2005

Thesis Advisor: Kyle T. Alfriend
Co-Advisor: Don A. Danielson

THIS PAGE INTENTIONALLY LEFT BLANK

REPORT DOCUMENTATION PAGE			Form Approved OMB No. 0704-0188
Public reporting burden for this collection of information is estimated to average 1 hour per response, including the time for reviewing instruction, searching existing data sources, gathering and maintaining the data needed, and completing and reviewing the collection of information. Send comments regarding this burden estimate or any other aspect of this collection of information, including suggestions for reducing this burden, to Washington headquarters Services, Directorate for Information Operations and Reports, 1215 Jefferson Davis Highway, Suite 1204, Arlington, VA 22202-4302, and to the Office of Management and Budget, Paperwork Reduction Project (0704-0188) Washington DC 20503.			
1. AGENCY USE ONLY ***(Leave blank)***	**2. REPORT DATE** September 2005	**3. REPORT TYPE AND DATES COVERED** Master's Thesis	
4. TITLE AND SUBTITLE: Orbit Determination of Highly Eccentric Orbits using a RAVEN Telescope		**5. FUNDING NUMBERS**	
6. AUTHOR(S) Thrall, Michael L.			
7. PERFORMING ORGANIZATION NAME(S) AND ADDRESS(ES) Naval Postgraduate School Monterey, CA 93943-5000		**8. PERFORMING ORGANIZATION REPORT NUMBER**	
9. SPONSORING /MONITORING AGENCY NAME(S) AND ADDRESS(ES) N/A		**10. SPONSORING/MONITORING AGENCY REPORT NUMBER**	
11. SUPPLEMENTARY NOTES The views expressed in this thesis are those of the author and do not reflect the official policy or position of the Department of Defense or the U.S. Government.			
12a. DISTRIBUTION / AVAILABILITY STATEMENT Approved for public release; distribution is unlimited.		**12b. DISTRIBUTION CODE**	

13. ABSTRACT (maximum 200 words)

For the past eight years, the small automated telescope Raven has been tested in detecting and tracking deep space objects. As the Raven has proven successful in tracking this regular and predictable orbit, its one arc-second accuracy made it a perfect candidate to attempt to accurately track the less predictable Highly Eccentric Orbit (HEO) objects. Ranging data was obtained from the Sirius satellite radio company for the Sirius3 satellite (Satellite Control Center (SCC) # 26626). This satellite was chosen for its long dwell time over the United States and for its favorable Raven tracking conditions. Angles-only data obtained from another Raven telescope located at the AMOS Remote Maui Experiment (RME) facility was used to track the satellite of interest. Then the Analytical Graphics, Inc. Satellite Tool Kit Orbit Determination (STK/OD) program was used to compare the accuracy of the orbit prediction using ranging tracking data from Sirius and angles-only tracking data from Raven. This paper shows the improvement in orbit determination uncertainty obtained by adding Raven observations to the ranging data. The Raven angles data improved the orbit plane uncertainty and eccentricity estimate differences by over 80% when used with the range observations.

14. SUBJECT TERMS RAVEN Telescope, Orbit Determination, HANDS, Sirius Satellite, Highly Eccentric Orbit			**15. NUMBER OF PAGES** 51
			16. PRICE CODE
17. SECURITY CLASSIFICATION OF REPORT Unclassified	**18. SECURITY CLASSIFICATION OF THIS PAGE** Unclassified	**19. SECURITY CLASSIFICATION OF ABSTRACT** Unclassified	**20. LIMITATION OF ABSTRACT** UL

NSN 7540-01-280-5500

Standard Form 298 (Rev. 2-89)
Prescribed by ANSI Std. 239-18

THIS PAGE INTENTIONALLY LEFT BLANK

Approved for public release; distribution is unlimited.

ORBIT DETERMINATION OF HIGHLY ECCENTRIC ORBITS USING A RAVEN TELESCOPE

Michael L. Thrall
Commander, United States Navy
B.S., United States Naval Academy, 1989

Submitted in partial fulfillment of the
requirements for the degree of

MASTER OF SCIENCE IN SPACE SYSTEMS OPERATIONS

from the

NAVAL POSTGRADUATE SCHOOL
September 2005

Author: Michael L. Thrall

Approved by: Kyle T. Alfriend
Thesis Advisor

Don A. Danielson
Co-Advisor

Rudy Panholzer
Chairman, Space Systems Academic Group

THIS PAGE INTENTIONALLY LEFT BLANK

ABSTRACT

For the past eight years, the small automated telescope Raven has been tested in detecting and tracking deep space objects. As the Raven has proven successful in tracking this regular and predictable orbit, its one arc-second accuracy made it a perfect candidate to attempt to accurately track the less predictable Highly Eccentric Orbit (HEO) objects. Ranging data was obtained from the Sirius satellite radio company for the Sirius3 satellite (Satellite Control Center (SCC) # 26626). This satellite was chosen for its long dwell time over the United States and for its favorable Raven tracking conditions. Angles-only data obtained from another Raven telescope located at the AMOS Remote Maui Experiment (RME) facility was used to track the satellite of interest. Then the Analytical Graphics, Inc. Satellite Tool Kit Orbit Determination (STK/OD) program was used to compare the accuracy of the orbit prediction using ranging tracking data from Sirius and angles-only tracking data from Raven. This paper shows the improvement in orbit determination uncertainty obtained by adding Raven observations to the ranging data. The Raven angles data improved the orbit plane uncertainty and eccentricity estimate differences by over 80% when used with the range observations.

THIS PAGE INTENTIONALLY LEFT BLANK

TABLE OF CONTENTS

I. INTRODUCTION 1
A. THE NEED FOR SPACE SURVEILLANCE 1
B. SPACE SURVEILLANCE 2
C. SPACE SURVEILLANCE NETWORK 3
D. HANDS 3
E. RAVEN TELESCOPE 4

II. BACKGROUND 7
A. RAVEN TELESCOPE 7
B. SIRIUS SATELLITE 8
C. STK/OD 10
1. Kalman Filter 11
2. Process Noise 11

III. ANALYSIS 13
A. OBSERVATIONS 13
B. DATA QUALITY TESTS 15
1. Orbit Determination Methods 17
2. Covariance 19
C. RESULTS 23

IV. CONCLUSIONS 25

APPENDIX A. STK/OD SCENARIO SETTINGS 27

LIST OF REFERENCES 33

INITIAL DISTRIBUTION LIST 35

THIS PAGE INTENTIONALLY LEFT BLANK

LIST OF FIGURES

Figure 1. JP 3-14 Space Control Matrix (From Ref. [1]) 2
Figure 2. HANDS Architecture/CONOPS (From Ref. [3]) 4
Figure 3. Sirius3 Ground Trace (From STK 6.1) 9
Figure 4. Sirius and RME Raven Observation Times 14
Figure 5. Sirius Range Only Residuals 15
Figure 6. Solar Radiation Pressure Estimate 16
Figure 7. Position Consistency Graph 17
Figure 8. Abutment Check 18

THIS PAGE INTENTIONALLY LEFT BLANK

LIST OF TABLES

Table 1. Metric Results Comparison 23

THIS PAGE INTENTIONALLY LEFT BLANK

ACKNOWLEDGMENTS

I would like to thank, first and foremost, Professor Kyle T. Alfriend. His leadership and willingness to aid in the study of this subject was of great inspiration. Secondly, I would like to thank Dr. Tom Kelecy of AMOS Maui, whose help with the Matlab and STK/OD programs made these results possible. Dr. Chris Sabol has also been a great help in the framing of the problem and for his unique insight of the Raven telescope. I would like to thank Dr. Paul Cefola of the Massachusetts Institute of Technology and Mr. Chris Croom of Sirius Satellite Radio Corporation, for sharing the satellite observation data with me. I would like to thank Professor Danielson for his help in the wording and flow of the thesis. I would also like to thank Analytical Graphics, Incorporated for allowing me use their Satellite Tool Kit and Satellite Tool Kit Orbit Determination software.

Also, I would like to thank the Air Force Office of Scientific Research (AFOSR) and the Air Force Research Lab's (AFRL) Extended HANDS program. Special thanks go to Dr. Clifford Rhoades of AFOSR and the Extended HANDS team.

THIS PAGE INTENTIONALLY LEFT BLANK

I. INTRODUCTION

A. THE NEED FOR SPACE SURVEILLANCE

The United States military's Joint Publication 3-14 (Joint Doctrine for Space Operations) provides guidelines for planning and conducting joint space operations. The Joint Chiefs of Staff (JCS) recognize space as a significant force multiplier for the United States military due to the reliance on space systems to carry out operations. In addition, the civil sector's reliance on space is a major factor in operations planning. Finally, it is recognized that current and future adversaries of the United States are dependent on their own space systems for intelligence collection against the United States.

To that end, the Joint Publication 3-14 mandates that the United States establish space superiority: "The use of space control operations to support freedom of action in space will ensure the ability to provide space capabilities to the warfighter and deny the opposing force the same."[1] In order to establish space superiority, four space missions must be accomplished: Space Control, Space Force Enhancement, Space Support, and Space Force Application. Since each of these mission areas is critical to achieving space superiority, they each have their own separate and distinct mission areas. Space Control operations "..provide freedom of action in space for friendly forces, while, when directed, denying it to an adversary, and include a broad aspect of protection of US and US allied space systems and degradation of adversary space systems."[2]

Space Control encompasses the following mission areas: Protection, Prevention, Negation and Surveillance. The following (Fig. 1) from JP 3-14 shows the relation of the four mission areas to space control[3]:

---

[1] Joint Pub 3-14, August 2002, p. IV-3.

[2] Ibid., p. IV-5.

[3] Ibid., p IV-7.

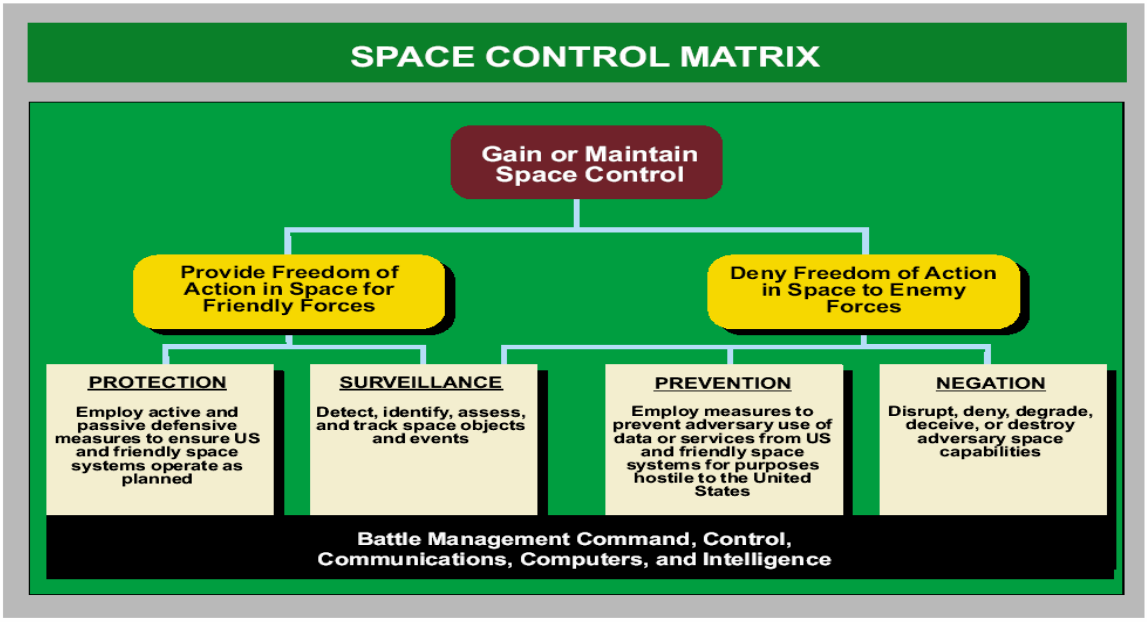

Figure 1. JP 3-14 Space Control Matrix (From Ref. [1])

B. SPACE SURVEILLANCE

While protection, prevention and negation are very important mission areas, this paper will focus on space surveillance. Space surveillance is deemed "fundamental to the ability to conduct the space control mission" and is defined as

> ..requiring robust space surveillance for continual awareness of orbiting objects; real-time search and targeting-quality information; threat detection, identification, and location…..conducted to detect, identify, assess, and track space objects and events to support space operations. Further, space situational awareness can be used to support terrestrially-based operations, such as reconnaissance avoidance and missile defense.[4]

It should be pointed out that space surveillance is critical to both providing freedom of action for friendly forces and denying freedom of action to enemy forces. It is the only mission area which affects both offensive and defensive sides of Space Control. By having a robust capability in space situational awareness, the United States will know when our forces are vulnerable to foreign

[4] Joint Pub 3-14, August 2002, p. IV-6.

intelligence-gathering space platforms in order to take timely and appropriate measures to defeat their attempts.

C. SPACE SURVEILLANCE NETWORK

As with any other surveillance technique or regime, the more accurate the data on the desired object, the better. In addition, minimizing the time and resources spent on obtaining highly accurate data is also a goal. This allows for a timely, clear picture of the battlespace, allowing the commanders more time to concentrate on avoiding or defeating the threat.

Current space situational awareness systems (e.g., the Air Force Space Surveillance Network (SSN)) are meeting space situational awareness requirements, but are doing so at great cost and take thousands of personnel to operate and maintain the systems throughout the world. The Space Surveillance Network is comprised of over forty radar and optical sites throughout the world, with the majority located in the Northern Hemisphere. In 2001, the Air Force spent over $60 million to operate the Space Surveillance Network[5]. In today's austere budget environment and with the age of the current SSN growing every year, it makes sense to investigate any and all ways to both increase accuracy and lower costs.

D. HANDS

One partial solution to this problem may be the High Accuracy Network Determination System (HANDS), a concept future network of optical telescopes that autonomously track both near-earth and deep space satellites and provide high accuracy orbit information.[6] Though HANDS is still in the development stage, the concept is to have thirty or more HANDS nodes spread throughout the world using automated telescopes to track earth orbiting objects of all regimes in conjunction with ranging data from selected SSN sites.

---

[5] Government Accounting Office Report GAO-02-403R, June 2002, p.2.

[6] Geosynchronous Orbit Determination Using HANDS, AAS 04-216, Sabol, Kelecy, Murai, February 2004, p. 1.

The angles data and ranging data are sent to the HANDS Operation Center by the Raven and AFSSN sites, where it is then fused and analyzed. The improved orbit estimates are then delivered to the customer. Fig. 2 below graphically illustrates the HANDS concept[7]:

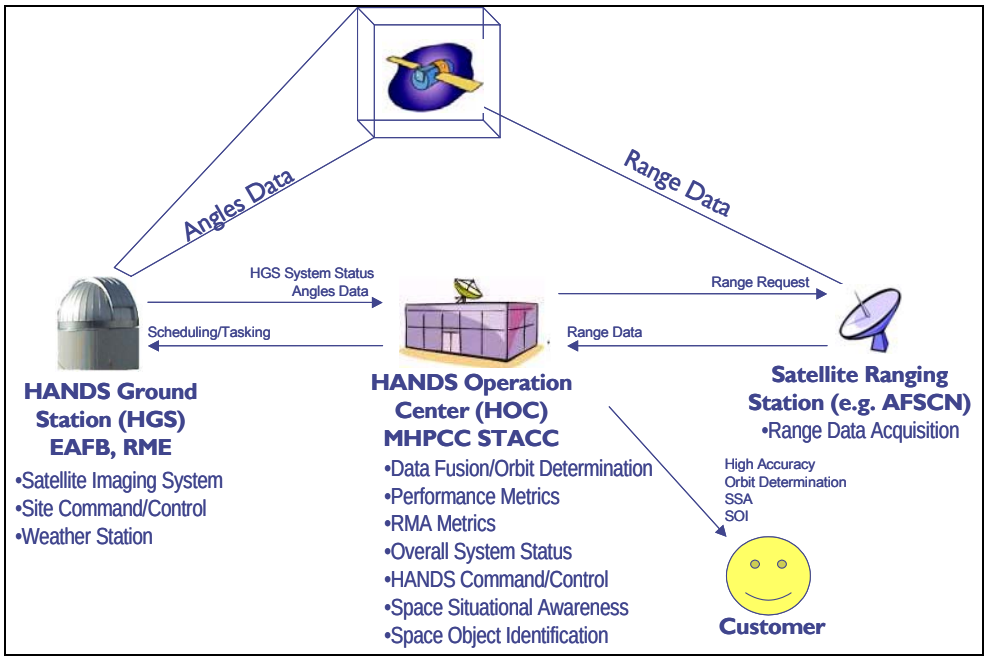

Figure 2. HANDS Architecture/CONOPS (From Ref. [3])

E. RAVEN TELESCOPE

The RAVEN telescope is planned to be the backbone of the HANDS network. RAVEN is a class of small telescopes that combine inexpensive commercial hardware with state of the art astrometric image reduction techniques to produce high accuracy angular observations of satellites[8].

The RAVEN telescope system is comprised of five major components: the 4 ft long telescope (0.37 meter mirror) and the dome which houses it, the telescope control computer, the Odin data processing workstation, the Global Positioning System (GPS) receiver and timing system, and a weather system

[7] Geosynchronous Orbit Determination using HANDS, AAS 04-216, Sabol, Kelecy, Murai, February 2004, p. 2.

[8] Recent Developments of the RAVEN Small Telescope Program, AAS 02-131, Sabol and others, January 2002, p.1.

which detects levels of wind, temperature, and humidity[9]. Raven telescope systems are designed to operate autonomously for weeks at a time without manual intervention[10].

This paper discusses the first trial of using the RAVEN telescope system for orbit determination accuracy against a HEO object. It will detail the object RAVEN tracked, the computer program used to determine Raven's accuracy, and the results using methods to differentiate between a range only solution and a range plus angles solution.

[9] Ibid, p. 7.

[10] Recent Developments of the RAVEN Small Telescope Program, AAS 02-131, Sabol and others, January 2002, p.12.

THIS PAGE INTENTIONALLY LEFT BLANK

II. BACKGROUND

A. RAVEN TELESCOPE

In the almost ten years since the Raven telescope prototype was built, Raven has become a very successful program. It has evolved from a good idea into a real-world Air Force Space Surveillance Network (SSN) sensor, capable of autonomously detecting, tracking and reporting geosynchronous objects with one arc-second accuracy. One Raven system is currently located at the summit of Mount Haleakala as a part of the Maui Space Surveillance Site (MSSS), providing space operators daily reports of deep space objects. A second system lies at the base of the mountain, in the Air Force Maui Optical and Supercomputing Site (AMOS) Remote Maui Experiment (RME) facility, hosting a large number of tracking experiments[11].

Due to Raven's documented success in tracking geosynchronous (GEO) objects with sub arc-second accuracy[12], it was decided to see how well it could track highly eccentric objects (HEO), which are typically more difficult to track and predict. HEOs typically have an inclination of 63.4 degrees so that perigee does not drift, and usually perigee is in the southern hemisphere. Since the SSN radars are in the northern hemisphere the HEO satellites are usually beyond the detection range of the radars. Then their high latitude in the northern hemisphere makes it more difficult to obtain optical observations. Depending on the eccentricity the primary perturbations may be different at perigee and apogee. For those with a low perigee the high velocity at perigee means that atmospheric drag can have a significant effect as it passes through perigee. All of these factors combine to make their orbit determination and prediction more difficult. Generally speaking, if an object has an eccentricity greater than 0.1, it is considered highly eccentric. The Raven telescope's accurate tracking of GEO

[11] Recent Developments of the RAVEN Small Telescope Program, AAS 02-131, Sabol and others, January 2002, p.2.

[12] High Accuracy Orbit Analysis Test Results Using HANDS, Kelecy, Sabol, and Murai, Sept 2003, p.9.

objects with one arc-second accuracy make it the perfect candidate to track the less predictable HEO objects.

B. SIRIUS SATELLITE

Though a Molniya-type orbit (e~0.7) is the most well-known of the highly eccentric orbits, access to current satellites flying in that orbit was not possible due to access to observations. To evaluate the effectiveness of the angle observations it is best to use a satellite with an accurate orbit. This allows one to compare the effectiveness of the orbit determination with angles only and with the addition of the angle observations to the primary observation set. The Sirius satellite radio constellation with an eccentricity of ~0.27 satisfied this criterion. There are three satellites in the Sirius constellation. Sirius3, (Space Control Center number 26626) was chosen due to its long dwell time over the United States and favorable tracking conditions, that is, it stays illuminated by the sun while Raven is in umber. Sirius3 has a 24-hour period (16 hours in the northern hemisphere), and is commanded and tracked by a facility located in Quito, Ecuador (Lat 0.273 deg S, Long 281.5 deg E, altitude 2604 m). Below is a quick synopsis of Sirius3's orbital elements and a ground trace (Fig. 3):

Epoch: 09 Dec 2004 03:30:47.475
Semi-major axis: 42165 km
Eccentricity: .268
True argument of latitude: 33.64 deg
Inclination: 63.83 deg
Right Ascension of the Ascending Node (RAAN): 29.82 deg
Argument of Perigee: 269.76 deg

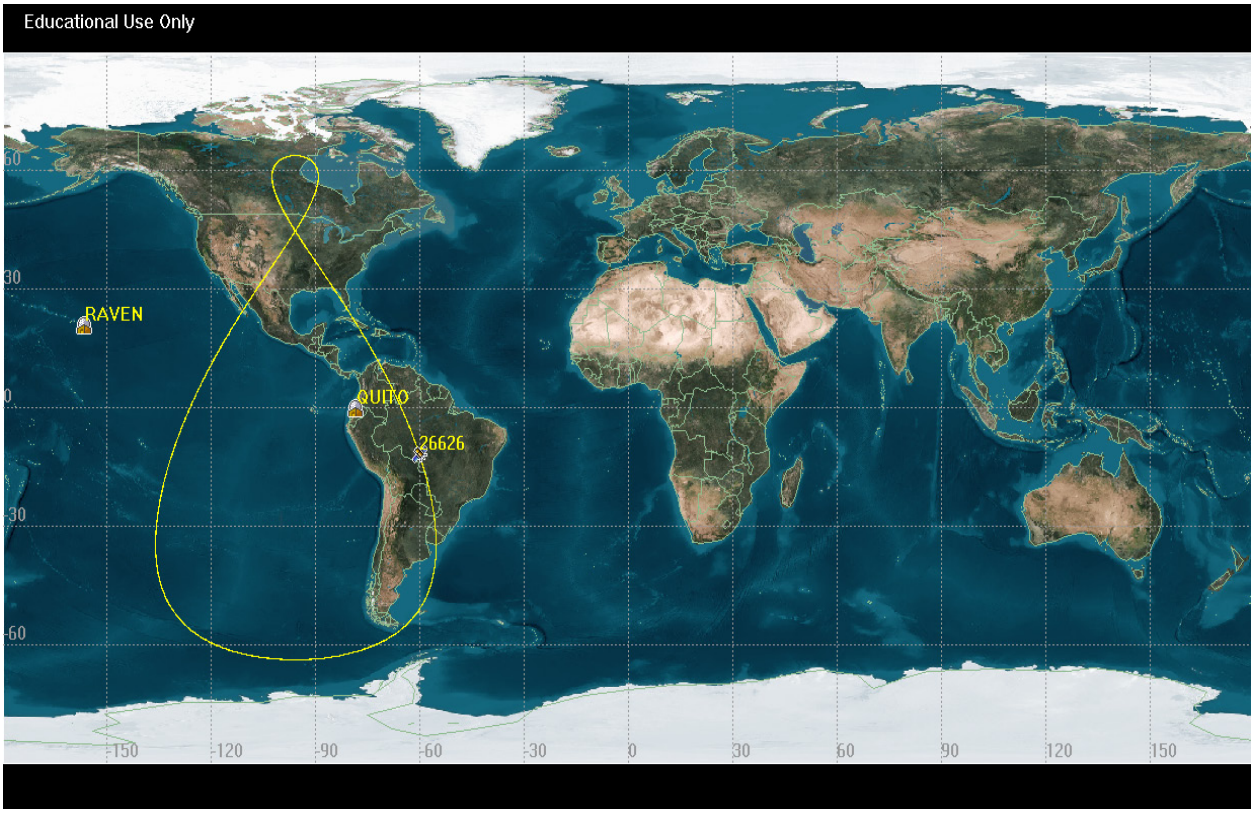

Figure 3. Sirius3 Ground Trace (From STK 6.1)

The 24-hour period and 63.4 degree inclination mean that the Sirius orbit is a double resonant orbit.

Through Massachusetts Institute of Technology (MIT), nearly constant (over the time period vice every second of that time period) tracking and telemetry data for the Sirius3 satellite were obtained. Dr. Paul Cefola of MIT and Mr. Chris Croom from Sirius provided files with range and angle observations. These observations were then converted to B3 format, necessary for computation in the orbit determination software. There were approximately four months of Sirius observations to use. The observations included both range and angle (azimuth and elevation) portions and covered a time period from December 4, 2004 through March 31, 2005. The Sirius angle observations are not very accurate, they help in the initial orbit determination, but their accuracy is not sufficient to improve in the maintenance of the orbit, i.e., the differential

correction. Consequently, they were only used in the initial orbit determination. Only ranging data were used in the analysis runs.

C. STK/OD

Analytical Graphic Incorporated's (AGI) Satellite Tool Kit/Orbit Determination version 3.0 (STK/OD) was used for processing the observations and determining the orbit. The program was responsible for all of the "heavy lifting" of data processing. However, testing of the software was completed to ensure comparable results from separate approaches before serious attention could be used on the results. The STK/OD output was compared against the industry-standard Goddard Trajectory Determination System (GTDS) program's output. Since GTDS is one of the recognized tools for orbit determination, settings in STK/OD were modified until output from STK/OD was similar to GTDS output.

Many runs were made in trying to get the settings in STK/OD to provide a consistent result against GTDS. Orbital elements, covariance, residual plots, solar radiation pressure (SRP) plots (dynamic in STK/OD, fixed in GTDS), and position consistency plots were some of the products compared to ensure consistency between STK/OD and GTDS. Each run was built using the five main subsets of a STK/OD scenario: tracking facility, initial orbit determination, filter, smoother, and satellite.

STK/OD requires that each scenario have the subsets listed above for every scenario run. The Initial Orbit Determination (IOD) is run first, using six angles (azimuth and elevation measurements at three different times) observations in order to compute a rough orbit. Once a rough orbit is generated, that orbit is transferred to the satellite. There is a least squares method that can be run to further refine the orbit with 10-20 of the initial observations, but it was decided that since the IOD was fairly close to the actual orbit, the least squares option did not need to be used.

1. Kalman Filter

STK/OD's filter is a forward-time recursive algorithm consisting of a repeating pattern of filter time updates of the state estimate, which propagates the state estimate forward, and filter measurement update of the state estimate which incorporates the next measurement. The filter uses the observations along with their location and a priori state estimate as the input, and provides optimal state estimates and realistic state error covariance matrices as the output, updated after every observation and at 1-second intervals[13]. The initial covariance is input as "orbit uncertainty", listed in the satellites settings. It is input in the radial, in-track, cross tack (RIC) reference frame. The only requirement for the initial covariance is that it not be too small, with many observations the final covariance is essentially independent of the initial covariance as long as it is not too small. Typically, it should be at least an order of magnitude larger than the expected final covariance. The only effect of a larger initial covariance is that the time to converge to a "steady state" covariance increases. For the runs, a diagonal covariance was used with 100,000 m for the RIC standard deviations and 100 m/sec for the RIC rate standard deviations.

2. Process Noise

In a Kalman filter implementation, process noise is used to represent the unmodeled accelerations and to prevent the covariances from getting too small. STK/OD has three types of process noise. To capture the gravitational force uncertainties and other unknown forces such as outgassing there is process noise in the radial, in-track and cross track directions (RIC). The magnitude in each of these three directions is an input quantity. In addition, there is process noise associated with both the solar radiation and atmospheric drag forces. Since the orbit's perigee was well above the atmospheric drag region (~29,500 km), atmospheric drag was not considered. The key question is what should the standard deviation of the process noise be, particularly with the different types of process noise. Due to the fact that a high order gravity model was used and lunar

[13] STK/OD manual.

and solar perturbations were included it was expected that the solar radiation pressure process noise would capture all the uncertainty. For the solar radiation the satellite was modeled as a sphere. To allow for the fact that the satellite is not a sphere an uncertainty in the two directions perpendicular to the satellite-sun line is allowed. This uncertainty is modeled as process noise with a magnitude of 0.3 times the solar radiation acceleration along the satellite-sun line with a half-life of 300 minutes. Including only solar radiation uncertainty was not sufficient, the residuals were too large. This was not due to station keeping maneuvers as a maneuver schedule was provided with the data and no maneuver was performed during the analysis time. Possibly some outgassing was occurring or there were momentum dumps that resulted in small linear accelerations that are caused by thruster mismatch. Therefore, it was necessary to include process noise in the RIC directions. A balance needed to be found between too much and too little unmodeled process noise in the satellite settings, and through numerous trials, it was found that a process noise of 0.01cm/s for each of the three RIC directions resulted in the necessary consistency in the residuals. Consequently, a process noise value of 0.01 cm/s was used for each axis.

III. ANALYSIS

A. OBSERVATIONS

A discussion of the observations is necessary before the analysis is presented. As discussed previously, observations were provided to AMOS from Sirius satellite radio via MIT. These observations were converted to the B3 format required for STK/OD. The Sirius observations in the month of December were fairly consistent, with an average of six observations per hour, spaced within a two minute timeframe, usually between :30 and :32 minutes past the hour, Greenwich Mean Time (GMT). An example of the raw Sirius observation data is below:

	Source	Ant	Type	Status	Data	Estimate	Noise	Residual
2004/12/09 15:30:22.264	c3_120920041530	QTB	range	accept	39325.0201 km	39367.1028 km	10.0000000 meters	-42082.6177 m
2004/12/09 15:30:24.300	c3_120920041530	QTB	azimuth	accept	305.698000 degs	305.059170 degs	0.0200000000 degs	0.638830439 degs
2004/12/09 15:30:24.300	c3_120920041530	QTB	elevation	accept	43.8500000 degs	43.5886859 degs	0.0200000000 degs	0.261314137 degs

The December Sirius observations were fairly consistent, except for some timeframes which were missing observations. Unfortunately, some of these timeframes coincided with the timing of the Raven observations. Fig. 4 below illustrates a timeframe in which there were gaps in Sirius observations (indicated by the TrackerID 999.00), coincident with Raven observations (shown as 998.1 and 998.2):

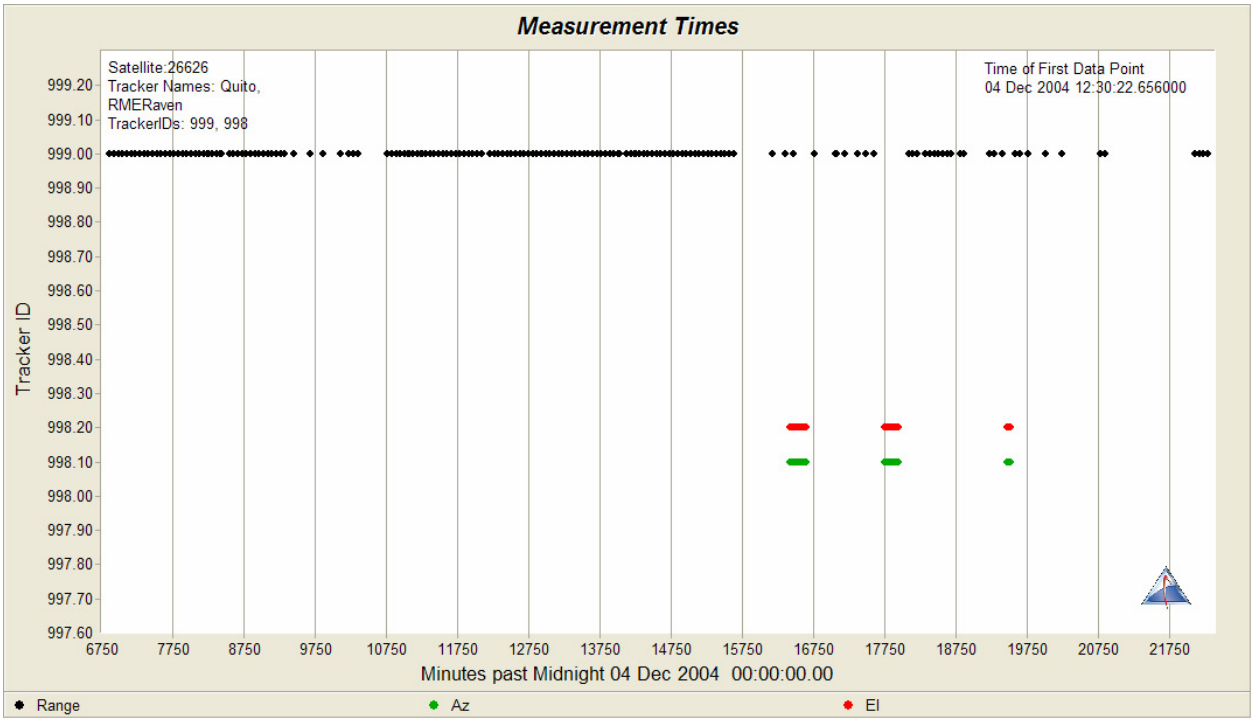

Figure 4. Sirius and RME Raven Observation Times

Though there were many observations collected by the AMOS Raven, located at the summit of Mount Haleakala, from December into January, these observations were not useable, due to shutter control issues. That left observations from the RME Raven, which was able to get approximately 200 observations of azimuth and elevation during the 15-17 December timeframe. These observations are the basis of the analysis[14], and there were enough observations to give a fairly clear picture of the results.

The majority of RME Raven observations were collected on 15-16 December, with ten observations of azimuth and elevation collected on 17 December. However, due to the exceptional one arc-second accuracy of the Raven telescope, the lack of observations is compensated by their accuracy.

[14] Observations made at the Maui Space Surveillance System (MSSS), Maui, Hawaii, USA are the result of collaboration between Dr. Chris Sabol and Detachment 15 of the US Air Force Research Laboratory, which owns and operates the MSSS.

B. DATA QUALITY TESTS

Once the observations were collected, an orbit had to be established in order to have a way of measuring improvement while determining the correct settings in STK/OD. The baseline orbit was chosen to be the Sirius orbit from 9-17 December, because of the number and quality of the range observations from the satellite. A number of tests were performed on the data to ensure the settings in STK/OD and the quality of observations were sufficient to establish the baseline orbit. One of these tests was the residuals check, shown in the graph in Fig. 5. A sigma of 10 meters was used for the Quito tracker. The residuals were consistent and reflected the expected result:

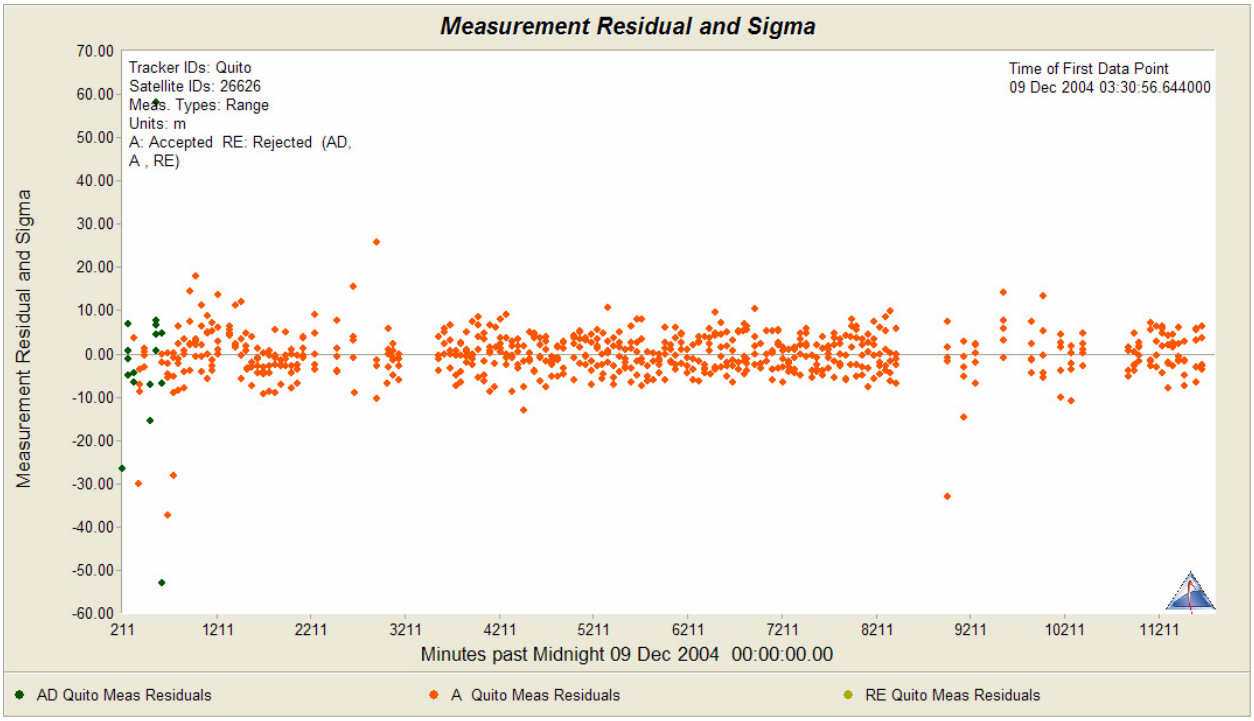

Figure 5. Sirius Range Only Residuals

Another test that was completed was to examine the Solar Radiation Pressure (SRP) dynamics plot. In STK/OD, the SRP estimate is shown as a correction to the estimated (input) value and the filter estimate. Since the Sirius orbit has an apogee of ~54,800 km, solar pressure on the satellite is a factor in orbit determination. To ensure an accurate solution, SRP was examined for any

perturbations which may skew the results. The figure below shows that SRP was consistent enough as to not affect the results. Both the SRP estimate and the +/- 2 sigma values are shown in Fig. 6.

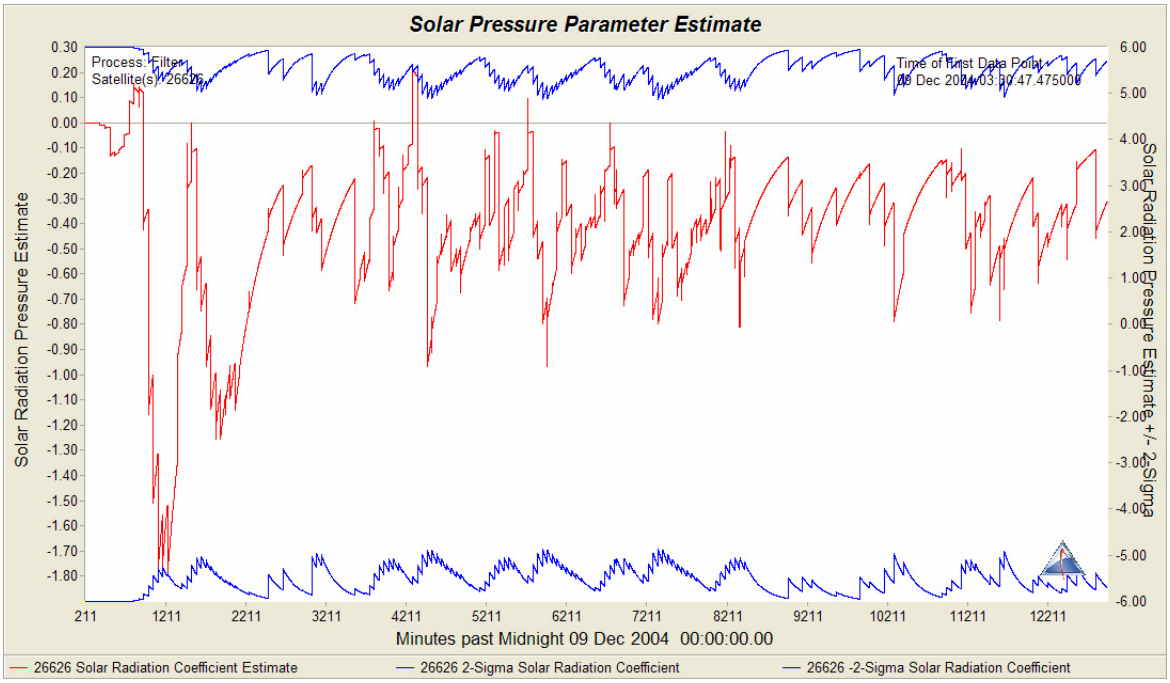

Figure 6. Solar Radiation Pressure Estimate

A final test for goodness was the comparison of the filtered run versus the smoothed run. The smoothed run is obtained by using the state and covariance at the final observation and performing a "backwards" filter with all the observations to obtain the optimal estimate during the span of data. This position consistency test ensures that the filter behaves as expected and there was not a large difference in the filtered results and the smoothed results. Fig. 7 shows the normalized differences of range, in-track, and cross-track results. The RIC values depicted in Fig. 7 show the difference in the filter run and the smoothed run using the McReynolds consistency test[15] found in STK/OD. The mean is zero, while the upper and lower bounds are +/- 3 sigma (dimensionless), visible at the upper and lower edges of the graph. Values within the +/- 3 sigma are considered reasonable.

[15] Optimal Orbit Determination, STK/OD White Paper, Wright, J., p.5.

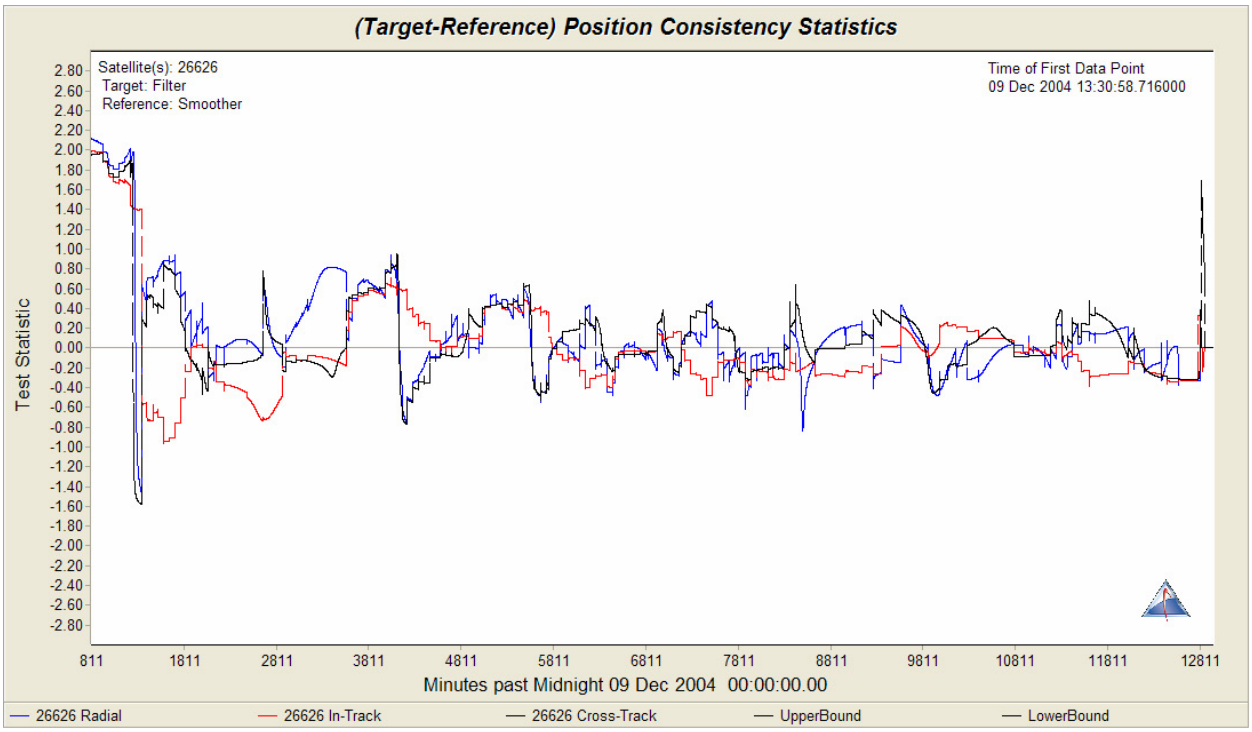

Figure 7. Position Consistency Graph

After establishing this orbit as the baseline orbit, the addition of the Raven observations and comparing the outputs of each was the next step. All settings in STK/OD were kept the same as they were for the Sirius observations only runs, with the exception of settings which added the Raven azimuth and elevation observations to the scenario. These settings can be seen in Appendix A.

1. Orbit Determination Methods

A measure of the quality of an orbit determination is the accuracy of the orbit prediction. The two primary approaches for determining this quality for different scenarios and sets of measurements are: (1) comparison of the actual orbit determination results, and (2) comparison of the covariances.

Comparing the accuracy of actual orbit determination results for different scenarios and sets of measurements of orbit determination is difficult when there

is no concrete truth orbit. One approach often used is to perform an “abutment check”, perform an orbit determination for two separate fit spans, then propagate the state from one epoch of one fit span across the other fit span, or if the fit spans are not contiguous propagate each orbit to a common time point between the two fit spans, and difference the results. This is shown graphically in Fig. 8 below:

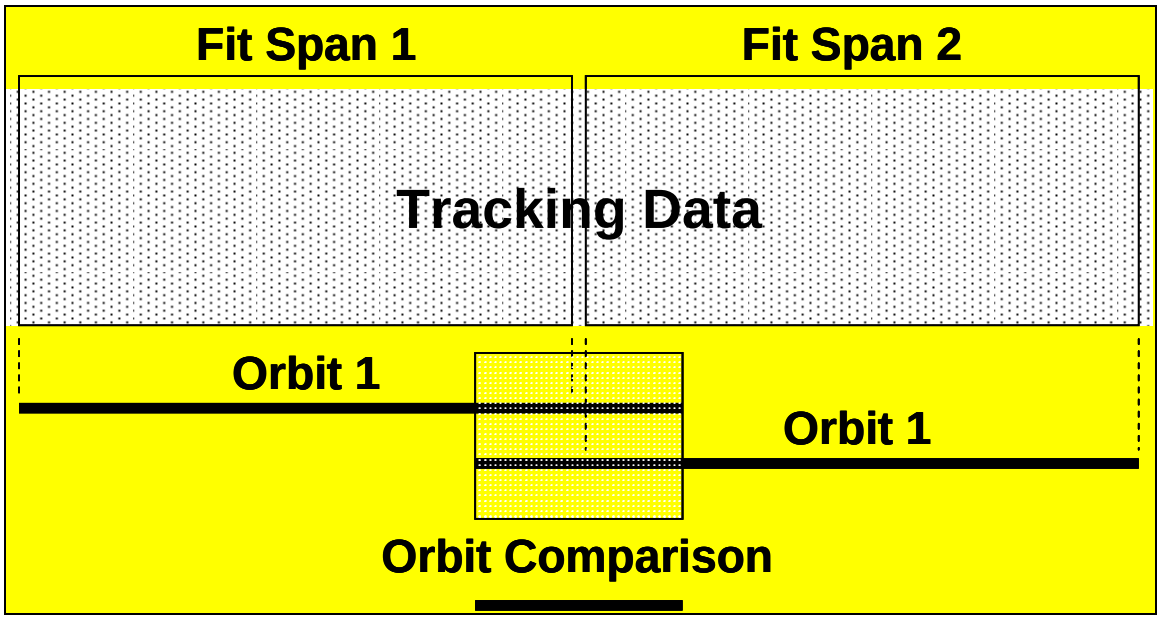

Figure 8. Abutment Check

If the orbit for the second fit span is truth, the difference is the error. If it is not truth, the problem becomes determining how to interpret the results. In the in-track direction, there is secular growth so if you predict long enough, this error will dominate the other errors during the fit span and one can assume the orbit during the fit span is truth. This is not the case for radial and cross-track comparisons because these errors are periodic and generally do not grow. Consequently, the comparison of real world results usually only works in the in-track direction. Since the “abutment check” is a comparison of actual results each case represents only one sample. To make any real conclusion from the “abutment check” there needs to be enough cases for a statistically reliable

sample. Unfortunately, the lack of angle observations over an extended period of time resulted in only one case, which prevented any meaningful comparison of the actual results in the in-track direction. Thus, the approach focused on comparing elements of the covariance.

2. Covariance

The covariance provides information on the accuracy of orbit determination. It can be used for comparison or just for a single fit. Of course, for the covariance to provide a valid assessment of the orbit determination accuracy, the modeling and sensors errors have to be accurately modeled. If one is comparing covariances, one can reasonably argue in some cases if both are in error in the same manner, the comparison is valid. For example, if the actual measurement errors for both fit spans are 5 arc-seconds, but are modeled as 10 arc-seconds, then the comparison should be valid.

After the last time step in the filter run, STK/OD outputs a covariance matrix in the radial, in-track, and cross-track (RIC) reference frame. The following are the filtered covariance and orbital elements outputs from the Sirius range only, and from the Sirius range plus Raven angles observations from the December 9-17 fit span:

Sirius Range-Only:	**Final Value**
Semimajor axis (km)	42164.509729
Eccentricity	0.268586659
True Arg of latitude (deg)	350.4501624
Inclination (deg)	63.8292837
Right Ascension of Ascending Node (RAAN) (deg)	29.6918866
Arg of Perigee (deg)	269.8341598

RIC Sigma Correlation Matrix (m & cm/s)

83.94 m	-0.86	0.92	0.89	-0.91	0.88
	660.34 m	-0.95	-1.00	0.98	-0.92
		546.94 m	0.95	-0.98	0.96
			5.90 cm/s	-0.98	0.92
				2.15 cm/s	-0.95
					2.22 cm/s

Sirius Range Plus Raven angles:	**Final Value**
Semimajor axis (km)	42164.492647
Eccentricity	0.26858577
True Arg of latitude (deg)	350.4477400
Inclination (deg)	63.8294392
Right Ascension of Ascending Node (RAAN) (deg)	29.6886020
Arg of Perigee (deg)	269.8303219

RIC Sigma Correlation Matrix (m & cm/s)

33.56 m	-0.01	0.32	0.34	-0.38	0.19
	121.60 m	0.00	-0.91	0.69	0.09
		65.76 m	-0.02	-0.40	0.60
			1.02 cm/s	-0.63	-0.08
				0.37 cm/s	-0.22
					0.52 cm/s

Here the following matrix is represented:

$$\begin{matrix} \sigma_X & \rho_{XY} & \rho_{XZ} & \rho_{X\dot{X}} & \rho_{X\dot{Y}} & \rho_{X\dot{Z}} \\ & \sigma_Y & \rho_{YZ} & \rho_{Y\dot{X}} & \rho_{Y\dot{Y}} & \rho_{Y\dot{Z}} \\ & & \sigma_Z & \rho_{Z\dot{X}} & \rho_{Z\dot{Y}} & \rho_{Z\dot{Z}} \\ & & & \sigma_{\dot{X}} & \rho_{\dot{X}\dot{Y}} & \rho_{\dot{X}\dot{Z}} \\ & & & & \sigma_{\dot{Y}} & \rho_{\dot{Y}\dot{Z}} \\ & & & & & \sigma_{\dot{Z}} \end{matrix}$$

Here, σ_X, σ_Y, and σ_Z denote the standard deviations of the radial error (X), in-track error (Y), and cross-track error (Z) and their rates of change $\left(\sigma_{\dot{X}}, \sigma_{\dot{Y}}, \sigma_{\dot{Z}}\right)$. ρ values are the correlation coefficients of the two values listed in the subscript of each ρ.

Making direct comparisons of these quantities provides no useful information because they are periodic and possibly secular. The in-track error growth rate (drift rate) is caused by a semi-major axis error. The radial error is caused primarily by an eccentricity error and the cross-track error is caused by

an error in the orbit plane estimate. The following equations[16] are taken from reference (7). The drift rate, *d*, is proportional to the semi-major axis error:

(1)

where δa is the semi-major axis error. The orbit plane error γ is given by

$$\gamma^2 = \delta i^2 + \left(\delta\Omega \sin i\right)^2 \tag{2}$$

where $(i, \delta i)$ are the inclination and inclination error, and, $\delta\Omega$ is the right ascension error. From ref [7], these quantities as a function of the RIC errors and error rates are

$$\begin{aligned}
\delta a &= \frac{2}{n\eta}\left[\left(e \sin f\right)\dot{X} + \left(1 + e\cos f\right)\dot{Y}\right] + \frac{2\left(1 + e\cos f\right)^2}{\eta^4} X \\
\delta e &= \left(\frac{2\eta^4}{e}\right)\left[\left(\frac{a}{R} - 1\right)\left(\frac{X}{R}\right) + \left(\frac{V_r}{V_c}\right)\left(\frac{\dot{X}}{V_c}\right) + \left(\frac{V_t}{V_c} - \frac{V_c}{V_t}\right)\left(\frac{\dot{Y}}{V_c}\right)\right] \\
\gamma^2 &= \frac{\left(V_t^2 + V_r^2\right)}{R^2 V_t^2} Z^2 + \frac{\dot{Z}^2}{V_t^2} - \frac{2V_r}{RV_t^2} Z\dot{Z}
\end{aligned} \tag{3}$$

where

$$\begin{aligned}
p &= a(1 - e^2) \\
R &= p/(1 + e\cos f) \\
\eta &= (1 - e^2)^{1/2} \\
h &= \sqrt{\mu p} \\
V_t &= (1 + e\cos f)(\sqrt{(\mu/p)}) \\
V_r &= (e\sin f)(\sqrt{(\mu/p)}) \\
V_c &= \sqrt{\mu/a}
\end{aligned} \tag{4}$$

[16] The State Transition Matrix of Relative Motion for the Perturbed Non-Circular Reference Orbit, by Gim, D. and Alfriend, K., *AIAA J. of Guidance, Control, and Dynamics*, Vol. 26, No. 6 November-December 2003, pp 956-971.

In equations (3) and (4), ($X,\dot{X}$) = radial, radial rate, ($Y,\dot{Y}$) = in-track, in-track rate, ($Z,\dot{Z}$) = cross-track, cross-track rate. V_t,V_r,V_c are the tangential, radial and circular velocities, respectively, p is the semi-latus rectum, R is the radius, a is the semi-major axis, h is the angular momentum, μ is the gravitational parameter, and f is the true anomaly.

The standard deviations of the quantities in equation (3) are

Semi-major Axis Error:

$$\sigma_{\delta a}=2a\left[\begin{array}{l}\left(\frac{V_r}{V_c}\right)^2\left(\frac{\sigma_{\dot{X}}}{V_c}\right)^2+\left(\frac{V_t}{V_c}\right)^2\left(\frac{\sigma_{\dot{Y}}}{V_c}\right)^2+\left(\frac{a}{R}\right)\left(\frac{\sigma_X}{R}\right)^2+ \\ 2\left(\frac{V_r}{V_c}\right)\left(\frac{V_t}{V_c}\right)\left(\frac{\sigma_{\dot{X}}}{V_c}\right)\left(\frac{\sigma_{\dot{Y}}}{V_c}\right)\rho_{\dot{X}\dot{Y}} \\ +2\left(\frac{V_r}{V_c}\right)\left(\frac{a}{R}\right)\left(\frac{\sigma_{\dot{X}}}{V_c}\right)\left(\frac{\sigma_X}{R}\right)\rho_{X\dot{X}}+2\left(\frac{V_t}{V_c}\right)\left(\frac{a}{R}\right)\left(\frac{\sigma_{\dot{Y}}}{V_c}\right)\left(\frac{\sigma_X}{R}\right)\rho_{X\dot{Y}}\end{array}\right]^{1/2} \tag{5}$$

Eccentricity Error:

$$\sigma_e=(2\eta^4/e)\left[\begin{array}{l}\left((\frac{a}{R})-1\right)^2\left(\frac{\sigma_X}{R}\right)^2+\left(\frac{V_r}{V_c}\right)^2\left(\frac{\sigma_{\dot{X}}}{V_c}\right)^2+\left(\left(\frac{V_t}{V_c}\right)-\left(\frac{V_c}{V_t}\right)\right)^2\left(\frac{\sigma_{\dot{Y}}}{V_c}\right)^2 \\ +2\left(\left(\frac{a}{R}\right)-1\right)\left(\frac{V_r}{V_c}\right)\left(\frac{\sigma_X}{R}\right)\left(\frac{\sigma_{\dot{X}}}{V_c}\right)\rho_{X\dot{X}} \\ +2\left(\left(\frac{a}{R}\right)-1\right)\left(\left(\frac{V_t}{V_c}\right)-\left(\frac{V_c}{V_t}\right)\right)\left(\frac{\sigma_X}{R}\right)\left(\frac{\sigma_{\dot{Y}}}{V_c}\right)\rho_{X\dot{Y}} \\ +2\left(\frac{V_r}{V_c}\right)\left(\left(\frac{V_t}{V_c}\right)-\left(\frac{V_c}{V_t}\right)\right)\left(\frac{\sigma_{\dot{X}}}{V_c}\right)\left(\frac{\sigma_{\dot{Y}}}{V_c}\right)\rho_{\dot{X}\dot{Y}}\end{array}\right]^{1/2} \tag{6}$$

Orbit Plane Error:

$$\sigma_{\gamma} = \left[\left(1 + \left(\frac{V_r}{V_t} \right)^2 \right) \left(\frac{\sigma_Z}{R} \right)^2 + \left(\frac{\sigma_{\dot{Z}}}{V_t} \right)^2 - 2 \left(\frac{V_r}{V_t} \right) \left(\frac{\sigma_Z}{R} \right) \left(\frac{\sigma_{\dot{Z}}}{V_t} \right) \rho_{Z\dot{Z}} \right]^{1/2} \quad (7)$$

C. RESULTS

Using the STK/OD provided classical orbital elements and covariance matrices, the numerical values for semi-major axis error, orbit plane error, and eccentricity error for the range only and the range and angles cases are summarized in Table (1) below.

Metric	Range Only	Range+Angles	Difference	Imp %
Semi-major-Axis Error (m)	**109.226**	**108.754**	**0.472**	**0.432%**
Orbit Plane Error (deg)	**0.000857**	**0.000127**	**0.000730**	**85.221%**
Eccentricity Error	**0.0000283**	**0.00000539**	**0.0000229**	**81.028%**

Table 1. Metric Results Comparison

What can be seen here is that there is a significant improvement of over 80% in both the orbit plane uncertainty and eccentricity estimate differences when Raven angles observations are used in conjunction with the range observations, even though there is only a very slight improvement in the semi-major axis error. This demonstrates that Raven angle observations improved the orbit determination parameters for this satellite.

THIS PAGE INTENTIONALLY LEFT BLANK

IV. CONCLUSIONS

The Raven telescope is a valuable asset to the space surveillance network, as it has already proved itself in tracking Geosynchronous satellites. Due to its accuracy, it was a natural fit to attempt to track (with the same orbit determination accuracy) Highly Eccentric Orbiting satellites. This study, though limited, has shown that Raven is ready to take the next step in completing the goal to track any deep space man-made object orbiting the earth. By strengthening the quality of the HEO object's orbit parameters, follow-on tracking is improved with a smaller search area for the object. This leads to better space situational awareness.

Because there was only three days of angles data, it was not possible to completely verify Raven could track HEO objects with the same accuracy. For this thesis, it would have been better to have a full week or more of Raven angle observations in which to build an orbit from, then to compare with a range only orbit. Abutment checks could have been completed and used for another proof of the increased orbit determination accuracy of the Raven telescope. However, based on the improvement in critical orbit metrics, this analysis makes a strong point for follow on testing against more objects in highly eccentric orbits.

For a complete evaluation of the angle observation contribution, a solid 30-day period of Raven angles observations would be enough to not only add to range only observations as done in this thesis, but to build an entirely new orbit. This new angle-only orbit could then be compared to a range-only orbit. If the two orbits compare favorably, it would indicate that the Raven could be a reliable sensor to track Highly Eccentric Orbits. There is more work to be done and all indications are that with enough data and sufficient documentation, HEO objects could then be added to Raven's object tracking list.

THIS PAGE INTENTIONALLY LEFT BLANK

APPENDIX A. STK/OD SCENARIO SETTINGS

1. FACILITY (Quito)

- **Position Geodetic**
  - **Lat** **-0.273042 deg**
  - **Lon** **281.524 deg**
  - **Alt** **2604 m**
- **Tracking ID** **999**
- **Estimate Nothing**
- **MinElevation** **5 deg**
- **MaxElevation** **90 deg**
- **RangingMethod** **Transponder**
- **AntennaType** **Mechanical**
- **Optical Properties**
  - **PolarExclusion** **1 deg**
  - **ReferenceFrame** **MEME of Date**
  - **AberrationCorrections** **None**
- **TroposphereModel**
  - **Enabled** **No**
  - **Model** **SCF**
- **TroposphereData**
  - **SurfaceRefractivity** **Constant**
  - **Value** **340**
- **IonosphereModel**
  - **Enabled** **No**
  - **Model** **IRI2001**
  - **TransmitFreq** **2267.5MHz**
  - **ReceiveFreq** **1815.77MHz**

2. FACILITY (RMERaven)

- **Position Geodetic**
  - **Lat** **20.7462 deg**
  - **Lon** **203.568 deg**
  - **Alt** **105.38 m**
- **Tracking ID** **998**
- **Estimate Nothing**
- **MinElevation** **5 deg**
- **MaxElevation** **90 deg**
- **RangingMethod** **SkinTrack**
- **AntennaType** **Optical**
- **Optical Properties**
  - **PolarExclusion** **1 deg**
  - **ReferenceFrame** **MEME J2000**
  - **AberrationCorrections** **None**
- **TroposphereModel**
  - **Enabled** **No**
  - **Model** **SCF**
- **TroposphereData**
  - **SurfaceRefractivity** **Constant**
  - **Value** **340**
- **IonosphereModel**
  - **Enabled** **No**
  - **Model** **IRI2001**
  - **TransmitFreq** **2267.5MHz**
  - **ReceiveFreq** **1815.77MHz**

3. INITIAL ORBIT DETERMINATION (IOD)

- **Method GoodingAnglesOnly**
  - **TrackerList Quito**
  - **StartTime 09 Dec 2004 00:00:00.000 UTCG**
  - **StopMode LastMeasurement**
  - **MeasurementSampleSize 300**
  - **MinimumElevation 5 deg**
  - **SelectedMeasurments Double click to edit**
  - **HalfRevEstimate 0**
  - **LambertIndicator 0**
  - **Range1Estimate 5 Re**
  - **Range3Estimate 5 Re**
  - **MaxIterations 25**
  - **ConvergenceValue 1e-012**
  - **HalleyNewtonLimit 0.5**
  - **NumericPartialEpsilon 1e-005**
  - **T12 7176.33 sec**
  - **T13 10742.2 sec**
- **Solutions**
  - **NumberOfSolutions 2**
  - **UseSolution 1**
- **Output**
  - **OrbitState Keplerian**
  - **CoordinateFrame J2000**

4. FILTER

- **ProcessControl**
  - **StartMode Initial**
  - **StartTime 9 Dec 2004 03:30:47.475 UTCG**
  - **StopMode StopTime**
  - **StopTime 31 Dec 2004 23:59:59.990 UTCG**
  - **ProcessNoiseUpdateInterval 1 min**
- **Restart**
  - **SaveRecordstoFile false**
  - **MaxRecordsinFile 100**
  - **SaveFrequency 60 min**
- **OptionalSolveForParms**
  - **MeasBiases true**
- **Output**
  - **DataArchive**
    - **OutputStateHistory AllTimes**
    - **EveryNSteps 1**
    - **SaveOnlyLastMeasPerStep false**
    - **OutputMeasHistory true**
    - **OutputManeuvers false**
    - **OutputSummary true**
    - **OutputHistograms true**
    - **HistogramSize 3**
    - **NumberHistorgramBins 22**
  - **Display**
    - **EveryNMeasUpdates 1**
    - **EveryNTimeUpdates 1**
    - **ShowPassTimes true**
  - **SmootherData**
    - **Generate true**
    - **TimeMode FilterSpan**
  - **STKEphemeris**
    - **DuringProcess**
      - **Generate false**
    - **Predict**

- **Generate false**

5. SMOOTHER

- **Input**
  - **Files double click to edit**
  - **Remove false**
- **ProcessControl**
  - **StartMode LatestFilterTime**
  - **StartTime 31 Dec 2004 23:59:59.990 UTCG**
  - **StopMode EarliestFilterTime**
  - **StopTime 9 Dec 2004 03:30:47.475 UTCG**
  - **OutputLag 0 min**
  - **IntervalLength 1440 min**
  - **IntervalOverlap 720 min**
- **Output**
  - **DataArchive**
    - **OutputStateHistory AllTimes**
    - **EveryNSteps 1**
    - **OutputManeuvers true**
  - **STKEphemeris**
    - **DuringProcess**
      - **Generate true**
      - **TimeGrid Filter**
    - **Predict**
      - **Generate true**
      - **TimeStep 1 min**
      - **StopMode TimeSpan**
      - **TimeSpan 720 min**
    - **Covariance true**
    - **CovarianceType position 3x3 Covariance**

6. SATELLITE

- **Description**
- **OrbitState Keplerian**
- **EstimateOrbit true**
- **OrbitClass LOeHEO**
- **PhysicalProperties**
  - **Mass 3000 kg**
- **MeasurementProcessing**
  - **TrackingID 26626**
  - **MeasurementTypes Range Azimuth Elevation**
  - **ResidualEditing**
    - **NominalSigma 3**
    - **Dynamic**
      - **Enabled true**
      - **HighSigma 10**
      - **NumRejectToStart 2**
      - **NumAcceptToStop 10**
      - **InitialHighSigmaDuration 120 min**
  - **ThinningTime 0 sec**
  - **MinPassDelta 20 min**
- **MeasurementStatistics None**
- **MinGrazingAlt 100000 m**
- **OpticalProperties**
  - **PolarExclusion 1 deg**
  - **ReferenceFrame MEME of Date**
  - **AberrationCorrections None**
- **RangingMethod Transponder**
- **IonosphereModel**
  - **Enabled false**
- **ForceModel**
  - **Gravity**
    - **DegreeandOrder 12**

- Tides
  - SolidTides false
  - OceanTides false
- GeneralRelativityCorrection false
- VariationalEquations
  - Degree 2
- ProcessNoise
  - Use BasedOnOrbitClass
  - WillUseProcessNoise true
  - OmissionErrorModeling
    - Enabled false
    - Scale 1
  - CommissionErrorModeling
    - Enabled false
    - Scale 1
  - ThirdBodies
    - Sun true
    - Moon true
    - Planets flase
    - UseinVariationaEquations false

- Drag
  - Use BasedOnOrbit
  - WillUseAirDrag false
- SolarPressure
  - Use BasedOnOrbit
  - WillUseSolarPressure true
  - EstimateSRP true
  - CPNominal 3
  - Area 38 m^2
  - CPInitialEstimate 0
  - CPHalfLife 300 min
  - ReflectionModel Sphere with diffuse reflection
  - SunPosMethod ApparentToTrueCB
  - UseInVariationalEquations true
  - AddProcessNoise true
  - EclipticNorthFraction 0.3
  - EclipticPlaneFraction 0.3
- Plugin
  - Use false
- UnmodeledAccelerations
  - ProcessNoise
    - RadialVelocitySigma 0.01 cm*sec^-1
    - IntrackVelocitySigma 0.01 cm*sec^-1
    - CrosstrackVelocitySigma 0.01 cm*sec^-1
    - TimeInterval 2 min
  - InstantManeuvers InstantManeuvers
  - FiniteManeuvers FiniteManeuvers
  - OrbitErrorTransitionMethod VariationalEquations

- PropagatorControls
  - IntegrationMethod RKF 7(8)
  - StepSize
    - Time .5 min
    - TrueAnomaly 2 deg
    - EccentricityThreshold 0.04
- EphemerisGeneration
  - CreateSTKFile false
- OrbitUncertainty
  - R_Sigma 100000 m
  - I_Sigma 100000 m
  - C_Sigma 100000 m
  - Rdot_Sigma 100 m*sec^-1
  - Idot_Sigma 100 m*sec^-1
  - Cdot_Sigma 100 m*sec^-1
  - AllCorrelations 0
- FilterEvents
  - MeasurementRejectThreshold
    - NumForWarning 0
    - NumForAlert 0
  - MeasurementAcceptTimer

- **TimeGapForWarning 0 min**

TimeGapForAlert 0

THIS PAGE INTENTIONALLY LEFT BLANK

LIST OF REFERENCES

1. *Joint Doctrine for Space Operations, JP 3-14*, Joint Staff, Washington, DC, August 2002.

2. *GAO Report 02-403R*, Government Accounting Office, Washington, DC June 2002.

3. *Geosynchronous Orbit Determination Using the High Accuracy Network Determination System (HANDS)*, AAS 04-216, by C. Sabol, T. Kelecy, and M. Murai, Air Force Research Lab, Maui, HI, January 2004.

4. *Recent Developments of the Raven Small Telescope Program*, AAS 02-131, by C. Sabol and others, Air Force Research Lab, Maui, HI, January 2002

5. *High Accuracy Orbit Analysis Test Results Using the High Accuracy Network Determination System (HANDS)*, by T. Kelecy, C. Sabol, and M. Murai, Center for Research Support, Schriever AFB, CO, September 2003

6. *Satellite Tool Kit Orbit Determination Software Help Manual*, Optimum Orbit Determination Definition

7. Gim, D. and Alfriend, K., "The State Transition Matrix of Relative Motion for the Perturbed Non-Circular Reference Orbit", *AIAA J. of Guidance, Control, and Dynamics*, Vol. 26, No. 6 November-December 2003

8. Wright, J. "Optimal Orbit Determination White Paper", [http://www.agi.com/pdf/white_papers/optimal_od.pdf]. 2003. Last accessed Sep 2005.

9. Vallado, D. and McClain, W., *Fundamentals of Astrodynamics and Applications*, 2nd ed., Microcosm Press, 2001.

THIS PAGE INTENTIONALLY LEFT BLANK

INITIAL DISTRIBUTION LIST

1. Defense Technical Information Center
   Ft. Belvoir, Virginia

2. Dudley Knox Library
   Naval Postgraduate School
   Monterey, California

3. Dr. Chris Sabol
   Air Force Research Laboratory
   Kihei, Hawaii

4. Analytical Graphics, Incorporated
   Valley Creek Corporate Center
   Exton, Pennsylvania